

# Evidence for particle-hole excitations in the triaxial strongly-deformed well of $^{163}\text{Tm}$

N.S. Pattabiraman<sup>1,2</sup>, Y. Gu<sup>1</sup>, S. Frauendorf<sup>1</sup>, U. Garg<sup>1</sup>, T. Li<sup>1</sup>,  
B.K. Nayak<sup>1</sup>, X. Wang<sup>1</sup>, S. Zhu<sup>1,3</sup>, S.S. Ghugre<sup>2</sup>, R.V.F. Janssens<sup>3</sup>,  
R.S. Chakrawarthy<sup>4</sup>, M. Whitehead<sup>4</sup>, and A.O. Macchiavelli<sup>5</sup>

<sup>1</sup> *Physics Department, University of Notre Dame, Notre Dame, IN 46556, USA*

<sup>2</sup> *UGC-DAE Consortium for Scientific Research,  
Kolkata Center, Kolkata 700 098, India*

<sup>3</sup> *Physics Division, Argonne National Laboratory, Argonne, IL 60439, USA*

<sup>4</sup> *Schuster Laboratory, University of Manchester, Manchester M13 9PL, UK*

<sup>5</sup> *Nuclear Science Division, Lawrence Berkeley  
National Laboratory, Berkeley, CA 94720, USA*

(Dated: June 25, 2018)

## Abstract

Two interacting, strongly-deformed triaxial (TSD) bands have been identified in the  $Z = 69$  nucleus  $^{163}\text{Tm}$ . This is the first time that interacting TSD bands have been observed in an element other than the  $Z = 71$  Lu nuclei, where wobbling bands have been previously identified. The observed TSD bands in  $^{163}\text{Tm}$  appear to be associated with particle-hole excitations, rather than wobbling. Tilted-Axis Cranking (TAC) calculations reproduce all experimental observables of these bands reasonably well and also provide an explanation for the presence of wobbling bands in the Lu nuclei, and their absence in the Tm isotopes.

PACS numbers: 21.10.Re; 21.60.Ev; 23.20.Lv; 27.60.+j

Stable asymmetric shapes have been a longstanding prediction of nuclear structure theory [1]. However, experimental evidence for such *triaxial* nuclei has proven difficult to establish. Still, triaxial shapes have been invoked to interpret a number of experimentally-observed nuclear structure phenomena such as signature inversion [2] and anomalous signature splittings [3], chiral twin bands [4], and, most recently, the wobbling mode [5]. Indeed, it has been generally agreed that the most convincing experimental evidence for stable triaxial shapes is provided by the wobbling mode, recently established in a number of odd-A Lutetium ( $Z = 71$ ) nuclei [6, 7, 8, 9, 10, 11, 12]. The nuclear wobbling motion, akin to the motion of an asymmetric top, is indicative of the three-dimensional nature of collective nuclear rotation [1]. In the quantum picture, the low-spin spectrum of such a system corresponds to that of the well-known Davydov asymmetric rotor. However, the low spin data do not allow a clear distinction between a rigid rotor and a system that is soft with respect to triaxial deformation. At high spins, the sequence of levels that can be associated with the excitation of wobbling phonons can be better distinguished from soft  $\gamma$  vibrations. The mode is evidenced in the Lu nuclei by families of strongly deformed (SD) triaxial rotational bands connected to one another and representing different wobbling phonon quantum numbers  $n_w$ ; bands up to  $n_w = 2$  have been observed thus far [8]. However, it has been surprising (and, indeed, somewhat frustrating) that in no other element has this mode been observed so far. Indeed, even though a number of SD bands have been reported in several nearby nuclei (up to 8 in case of  $^{174}\text{Hf}$ !), many of which may be grouped into possible families based on similarities of their dynamic moments of inertia, there has been no evidence for connecting transitions between these bands [13, 14]. Such connecting transitions are a *sine qua non* condition of wobbling bands and strong  $\Delta J = 1(0)$ ,  $E2$  linking transitions between the  $n_w + 1$  ( $n_w + 2$ ) and  $n_w$  wobbling partners are expected to occur over a large spin range.

We report the observation of two SD bands in the  $Z = 69$  nucleus  $^{163}\text{Tm}$ , an isobar of  $^{163}\text{Lu}$ , the nucleus with the most extensive experimental evidence for wobbling bands [8]. We have identified several transitions connecting the two bands; however, these are unlike the characteristic transitions between wobbling bands and, instead, are akin to a “particle-hole excitation”. Still, this is the first time that two triaxial SD bands with interconnecting transitions have been observed in any element other than Lu. The properties of these bands are well reproduced by calculations in the framework of the Tilted-Axis Cranking (TAC) model. Moreover, the calculations provide an explanation of why one observes particle-hole

excitations in the Tm nuclei, but wobbling in the Lu isotopes.

High spin states in  $^{163}\text{Tm}$  were populated via the  $^{130}\text{Te}(^{37}\text{Cl},4n)^{163}\text{Tm}$  reaction, at a bombarding energy of 170 MeV. The beam was provided by the 88-inch cyclotron facility at the Lawrence Berkeley National Laboratory. A self-supporting, isotopically enriched target-foil of about  $0.5\text{ mg/cm}^2$ -thickness was used. To prevent contamination and degradation of the target, it was coated with an Aluminum layer, about  $0.04\text{ mg/cm}^2$ -thick, on both sides. Quintuple- and higher-fold coincidence events were recorded with the Gammasphere array [15]; at the time of the experiment, the array had 98 active Compton-suppressed HPGe detectors. A total of about one billion events was accumulated and stored onto magnetic tapes for further analysis. The data-analysis procedures for developing the level schemes from Gammasphere data, and for assignments of spins and parities based on DCO ratio measurements, are more-or-less standard by now and only the most pertinent details are provided here. The data were sorted into three-dimensional and four-dimensional histograms [16, 17] and analyzed by projecting double- and triple-gated coincidence spectra. The analysis has resulted in extensive development of the level scheme of  $^{163}\text{Tm}$ ; a partial level scheme, relevant to the subject matter of this Letter, is presented in Fig. 1. Supporting coincidence

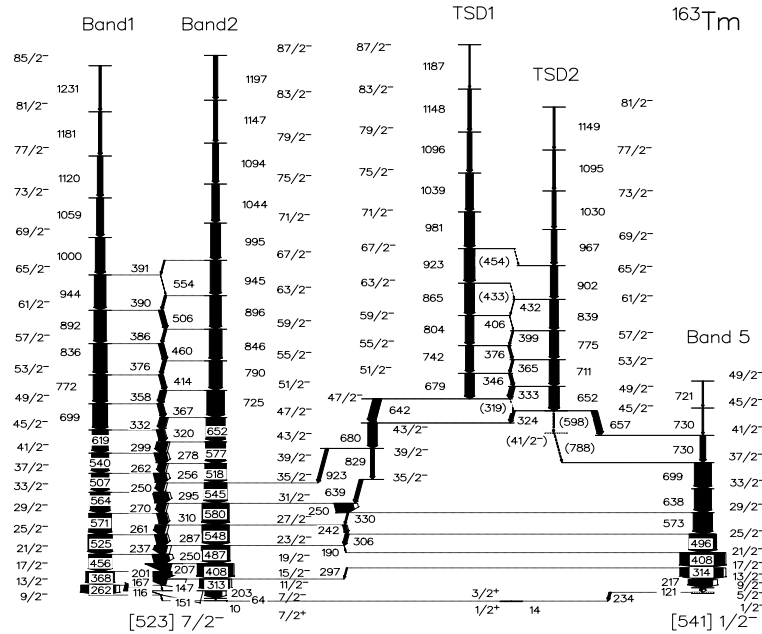


FIG. 1: Partial level scheme of  $^{163}\text{Tm}$ , showing the TSD bands, their interaction, and feeding to normal deformed bands. The transition intensities are proportional to the thickness of the arrows.

spectra are illustrated in Fig. 2: the top and middle panels show, respectively, the  $\gamma$ -ray transitions in the sequences labeled TSD1 and TSD2, with an energy spacing  $\Delta E \sim 60$  keV; the bottom panel displays many of the “connecting” transitions in coincidence with the bands. Each of these bands is of about 2-3% of the total intensity in  $^{163}\text{Tm}$ .

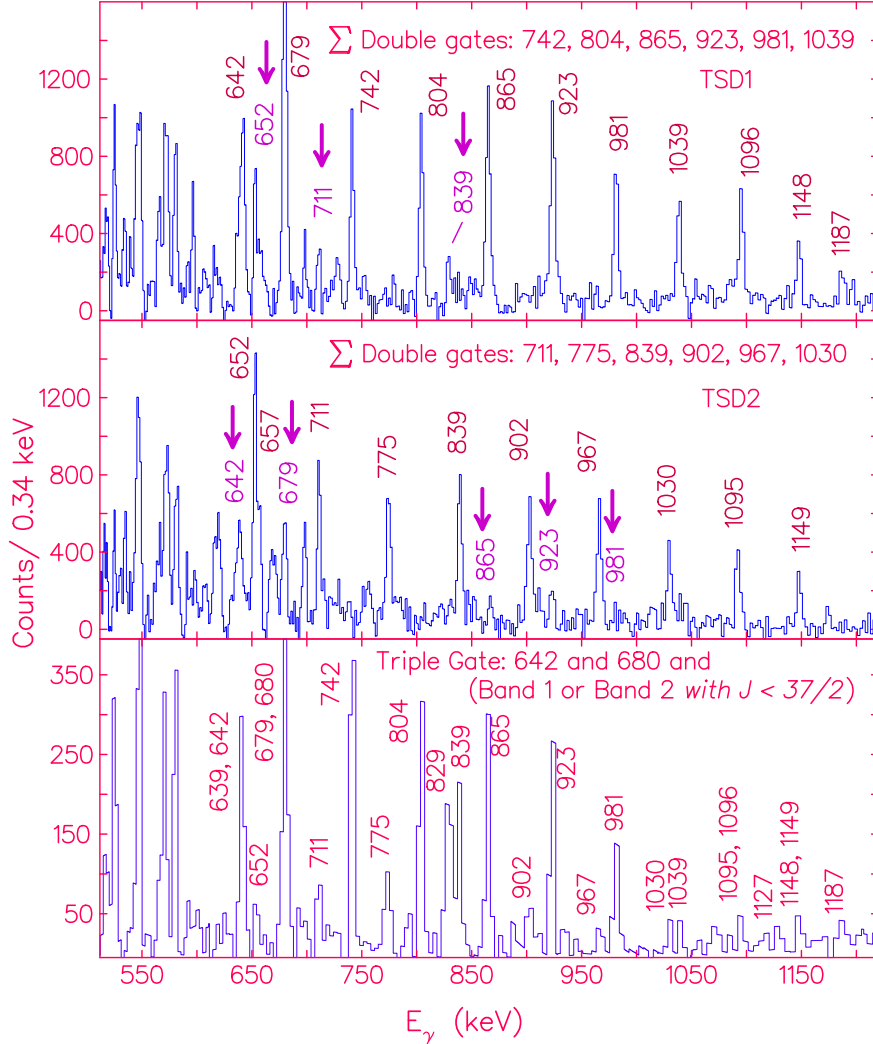


FIG. 2: Background subtracted coincidence spectra in  $^{163}\text{Tm}$  from the summation of spectra with double gates set on bands TSD1 (top panel) and TSD2 (middle panel), respectively. The arrows indicate the appearance of transitions from TSD2 in the TSD1 spectrum, and *vice versa*. The bottom panel provides further evidence for the “connecting” transitions.

Angular correlation analyses helped in ascertaining the  $\Delta J = 2$  character of the transitions in these bands; they have all been assigned an  $E2$  multipolarity. The linking transitions

are found to be  $\Delta J = 1$  in character, with small possible admixtures, and have been assumed to be of  $M1$  multipolarity. The spin and parity quantum numbers of the two bands are established on the basis of the multiplicities of the transitions linking them to the previously-known states in this nucleus [18]. With the established level scheme and the proposed multipolarity assignments, the alignments,  $i_x$ , and the dynamic moment of inertia,  $J^{(2)}$ , have been calculated and are plotted as a function of rotational frequency in the Fig. 3. These plots suggest that the properties of these bands are very similar to those

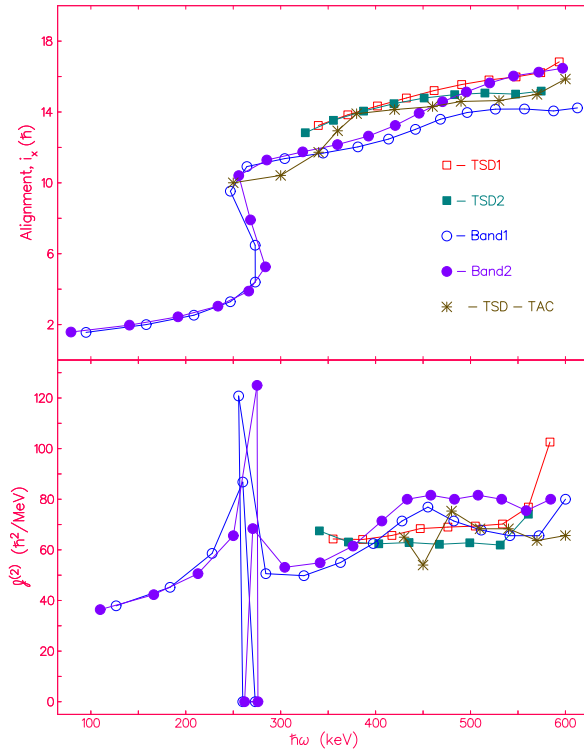


FIG. 3: Alignments  $i_x$  (upper panel) and the experimental dynamic moments of inertia  $J^{(2)}$  (lower panel) for the two TSD bands in  $^{163}\text{Tm}$  as a function of rotational frequency. The reference for the alignment is  $I_{ref} = \mathfrak{S}_0\omega + \mathfrak{S}_1\omega^3$  with  $\mathfrak{S}_0 = 30\hbar^2 \text{ MeV}^{-1}$  and  $\mathfrak{S}_1 = 40\hbar^2 \text{ MeV}^{-3}$ . The calculated alignments and the dynamic moments of inertia for the TSD bands in the TAC model are also shown.

of other triaxial strongly-deformed (TSD) bands observed in this region and, thus, have triaxial deformation similarly. Their SD nature has been established in a separate DSAM measurement [19], where the average associated transition quadrupole moments were found to be  $Q_t \sim 8.5 \text{ eb}$  in both bands. We note that, although the dynamic moments of inertia associated with the yrast bands (labeled Band1 and Band2 in Figs. 1 and 3) are very similar

to those in TSD1 and TSD2, the DSAM measurements [19] indicate that their associated  $Q_t$  moments are significantly smaller ( $\sim 6$  eb).

Fig. 4 shows the excitation energies of these TSD bands relative to a rigid rotor reference. The exhibited pattern is quite different from that observed in the case of wobbling bands (see, for example, Fig. 14 in Ref. [7]), and is indicative of the very different nuclear structure associated with these bands. Another major difference from the wobbling bands is that the transitions between TSD1 and TSD2 are “interconnecting”, *i.e.*, there are linking transitions going *both* ways between the two bands, whereas for the wobblers the connecting transitions always proceed only from the band with a higher  $n_w$  value to that with a lower  $n_w$ .

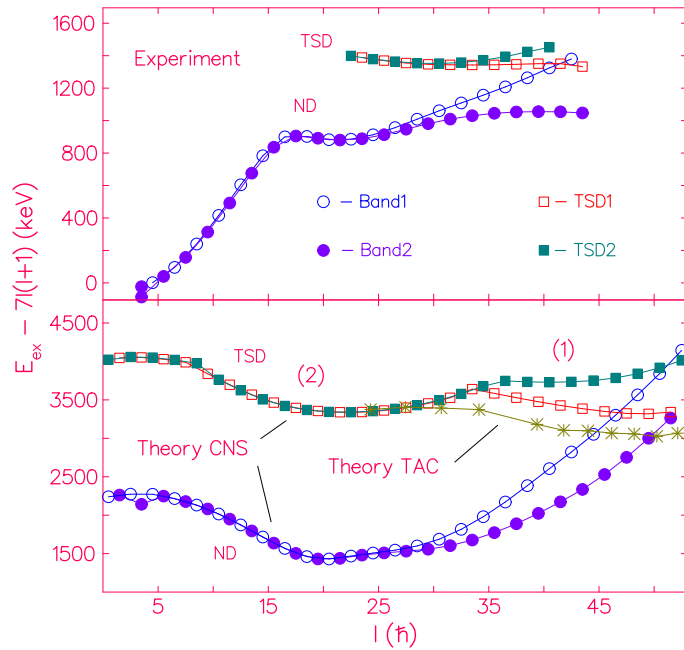


FIG. 4: Excitation energies relative to a rotational reference for the two TSD bands and the normal-deformed structures (Band1 and Band2) in  $^{163}\text{Tm}$ . The top panel shows the experimental energies. The energies calculated by means of CNS and TAC models are presented in the bottom panel. The numbers (1) and (2) with the CNS calculation indicate the associated minima from Fig. 5 (minimum 1 has  $\gamma > 0^\circ$  and minimum 2 has  $\gamma < 0^\circ$ ).

To understand the observed properties of these bands and their distinct differences from the sequences in the Lu nuclei, we have performed calculations in the frameworks of the configuration-dependent Cranked Nilsson-Strutinsky (CNS) model [20] and the Tilted-Axis

Cranking model (TAC, Shell Correction version SCTAC) [21]. The CNS model is a special case of the TAC approach assuming that the axis of rotation is one of the principal axes. If this axis turns out to be stable, CNS calculations provide a solution of the TAC problem. If it is unstable, one has to use the TAC code to find the tilted solution. The technically simpler CNS calculations were carried out first, using the parameters advocated in Ref. [20] for the deformed mean field. The same set was subsequently used for the TAC calculations. Pairing was assumed to be zero; CNS calculations without pairing have been successfully applied in numerous cases in the spin range considered here [22].

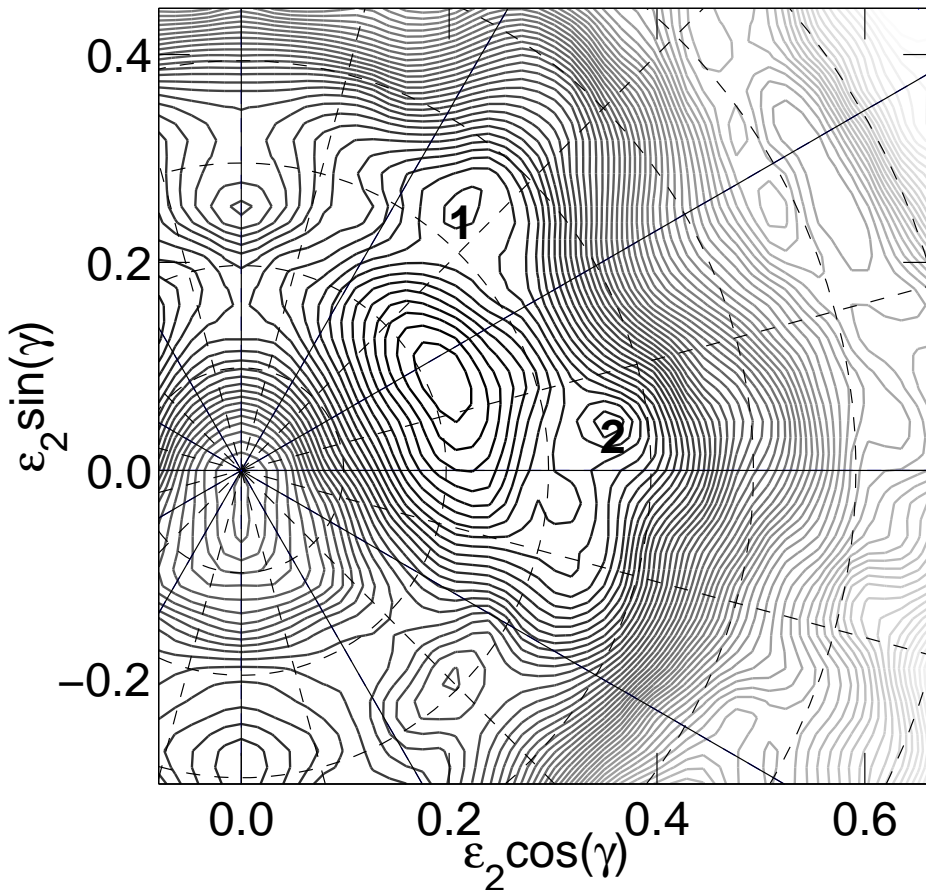


FIG. 5: Potential Energy surface for  $^{163}\text{Tm}$  calculated by means of the CNS model at  $I^\pi = 63/2^-$ . The two TSD minima are marked by 1 and 2. The energy step between the contours is 0.25 MeV.

Fig. 5 presents the CNS energy of a configuration with  $(\pi, \alpha) = (-, -1/2)$  (see details below) as function of the deformation  $\epsilon_2$  and the triaxility parameter  $\gamma$  for  $I^\pi = 63/2^-$ . Similar to Ultimate Cranker calculations in Refs. [6, 7, 8, 9, 10, 11, 12, 23], the CNS model

gives a prolate minimum at normal deformation ( $\varepsilon \approx 0.21$ ), which we refer to as ND, and two triaxial strongly deformed minima, which we refer to as TSD. It is worth pointing out that, in contrast with previous calculations with  $Z > 69$  and  $N \sim 94$  [6, 7, 8, 9, 10, 11, 12], the  $i_{13/2}$  proton level is empty in  $^{163}\text{Tm}$ , which means that this level is not essential in forming the TSD minima. Rather, it is the gap in the neutron spectrum at  $\varepsilon_2 \approx 0.39$ ,  $|\gamma| \approx 17^\circ$  which stabilizes the TSD shape (*cf.* Ref. [23], Fig. 3).

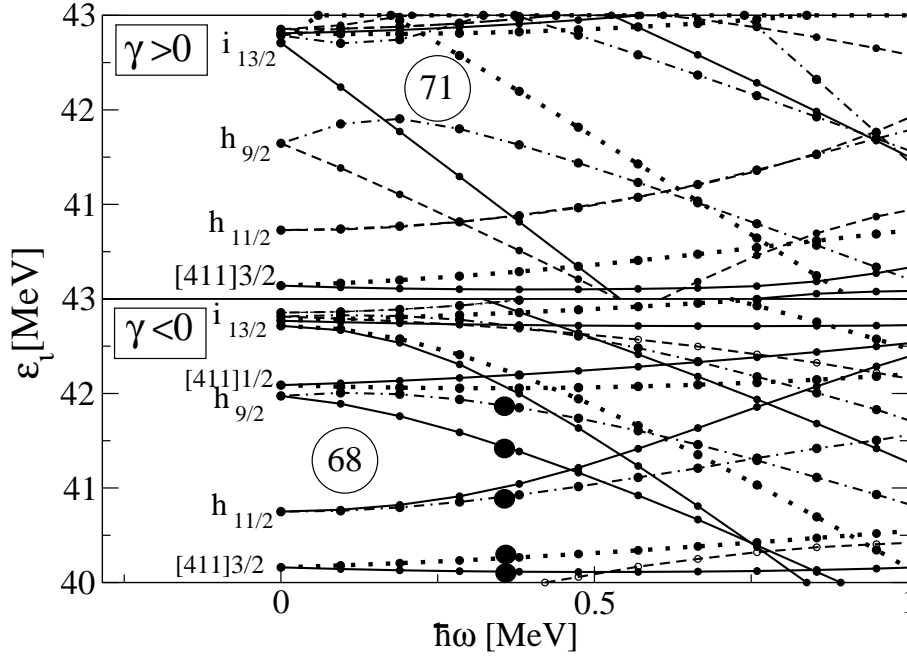


FIG. 6: Single-proton routhians as function of rotational frequency in TSD minima 1(top) and 2 (bottom). The line convention is  $(\pi, \alpha) = (+, 1/2)$  full,  $(+, -1/2)$  dot,  $(-, 1/2)$  dash,  $(-, -1/2)$  dash dot. Large filled circles mark occupied levels.

Fig. 6 presents the single proton routhians in both of the TSD minima. The TSD configuration that we assign to the observed band TSD1 is indicated by the large filled circles on the occupied levels. It is the lowest configuration with negative parity and small signature splitting. There are competing configurations with similar energy, which will be discussed below. The single-proton routhians in the ND minimum (not shown) look similar to the ones of Fig. 6, except that the  $h_{11/2}$  orbital has a larger splitting between the two signatures, as expected for the associated smaller deformation. We interpret bands 1 and 2 after the backbend as the two signatures of the odd proton occupying the  $h_{11/2}$  level at the



Fermi surface. In contrast to the TSD configuration, the proton pair on the  $h_{9/2}$  routhians is placed on the  $[411]_{1/2}$  routhians in the ND configuration. Fig. 4 compares the calculated and experimental energies. The observed substantial signature splitting is consistent with the calculation. The measured transition quadrupole moment  $Q_t$  for ND bands of  $\sim 6$  eb agrees well with the CNS calculation, which gives values around 6.5 eb.

As seen in Fig. 5, the two TSD minima have nearly the same energy. It is clear from the bottom panel of Fig. 4 that minimum 2 is energetically favored at low spin and minimum 1 at high spin. The two minima have almost the same value of  $\epsilon$  and  $|\gamma|$ , indicating that both are associated with the same shape. The axis of rotation is the short one in minimum 1 (with  $\gamma > 0^\circ$ ), while it is the intermediate one for minimum 2 (with  $\gamma < 0^\circ$ ). Thus, the CNS calculations suggest that at  $I = 24\hbar$ , where minimum 1 goes below minimum 2, the orientation of the rotational axis flips from the intermediate to the short axis. This sudden flip is caused by the inherent assumption in the CNS model that the rotational axis must be a principal one, and in fact indicates that this assumption of rotation about a principal axis is inappropriate. Therefore, TAC calculations, which do not restrict the orientation of the rotational axis, were carried out. As expected, a tilted solution with lower energy was found, which smoothly connects minimum 2 with minimum 1. For  $I > 23$  the angular momentum vector moves away from the intermediate axis toward the short axis. It does not quite reach it within the considered spin range. (For  $I \sim 50$ , the angle with the intermediate axis is still about  $20^\circ$ .) This solution is assigned to bands TSD1 and TSD2. In accordance with the experiment, it corresponds to a  $\Delta I = 1$  band without signature splitting. The observed onset of signature splitting at the highest spins is consistent with the calculated approach of the TAC solution to minimum 1 of the CNS result. At large frequency, the calculated TSD bands have a lower energy than the ND ones, which is consistent with the experiment whereby Band 1 crosses TSD1 at the highest spins. The TAC calculations for TSD bands give values of the transition quadrupole moment that increase slightly from 8.7 eb at  $I = 24$  to  $\sim 9.6$  eb for  $34 < I < 50$ , in agreement with the experimental values  $Q_t \sim 8.5$  eb. Furthermore, as seen in Fig. 7, the calculated B(M1)/B(E2) ratios of TSD bands agree well with experimental values. Finally, Fig. 3 demonstrates that the calculations also reproduce the experimental alignments and the dynamic moments of inertia  $J^{(2)}$  very well. Thus, all experimental observables for the TSD bands are accounted for by the TAC calculations.

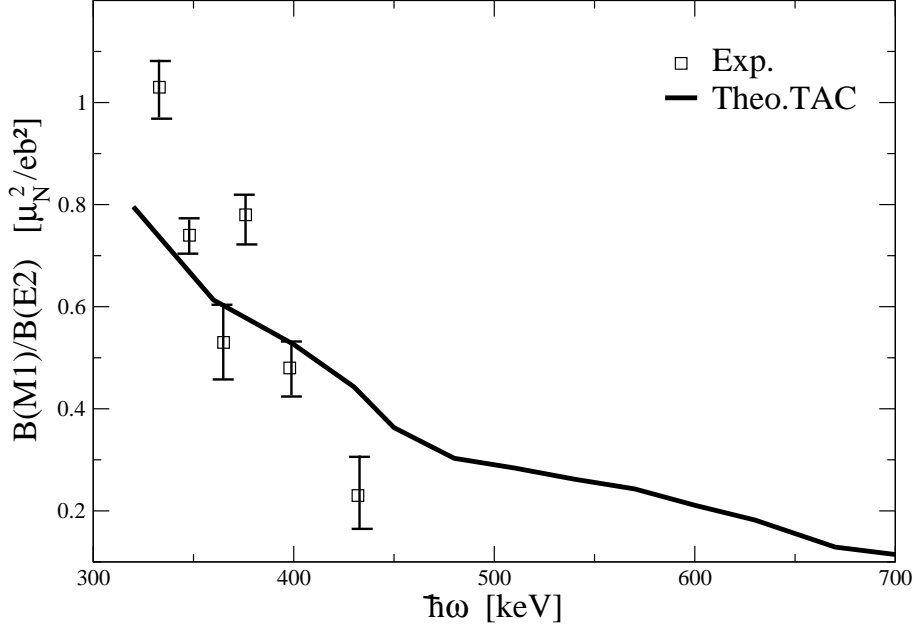


FIG. 7:  $B(M1)/B(E2)$  values as a function of the rotational frequency for the TSD bands. Squares with error bars are experimental data; the solid line is the TAC calculation described in the text.

The configurations that we assign to the bands TSD1 and TSD2 (indicated by the large filled circles in Fig. 6) are the lowest with negative parity and small signature splitting, in agreement with the experiment. The CNS calculations also predict four other TSD configurations (termed TSD3, TSD4, TSD5, and TSD6 in the discussion below) at somewhat lower energy than TSD1 and TSD2. The positive-parity configurations TSD3 and TSD4 have the odd proton on one of the  $[411]_{1/2}$  routhians and have both  $h_{11/2}$  signatures occupied; they are predicted by the CNS calculations to lie about 500 keV below TSD1 at spin 20 and have a larger energy above spin 50. However, as can be seen in Fig. 10 of Ref. [18], some residual proton pair correlations in the lower-spin part will disfavor the configurations TSD3 and TSD4 with respect to TSD1 and TSD2. The configurations TSD5 and TSD6, with both signatures of the  $h_{11/2}$  orbital occupied and the odd proton on one of the two  $h_{9/2}$  routhians, would correspond to two well-separated  $\Delta I = 2$  sequences with little resemblance to the experiment. The favored signature branch, TSD5, is predicted by the CNS calculations to lie about 500 keV below TSD1 at spin 20 and to have a larger energy than TSD1 above spin 40. We note here that the location of the  $h_{9/2}$  orbital has been a longstanding open problem in calculations using the modified oscillator potential (*cf.* the discussion in Ref. [18]). On the other hand, Ref. [24] demonstrated that the Woods-Saxon potential (universal parameters)

reproduces the position of this orbital well for normal deformations. A calculation using the hybrid version of TAC [25], which is a good approximation of the Woods-Saxon potential, with  $\epsilon_2 = 0.4$ ,  $\epsilon_4 = 0.04$ , and  $\gamma = 17^\circ$ , all choices close to the self-consistent values, places TSD1 and TSD2 at about the same energy as TSD4 and TSD5 for the low spins, and below them for the higher spins. This points to possible problems with the modified oscillator potential for the TSD shapes which appear to be absent in the Woods-Saxon potential.

The single particle routhians in Fig. 6 provide a natural explanation for the presence of collective wobbling excitations in the Lu isotopes with  $Z = 71$  and their absence in  $^{163}\text{Tm}$  with  $Z = 69$ . The TSD configurations of nuclei with  $Z > 69$  belong typically to minimum 1 with  $\gamma > 0^\circ$  [23]. For  $Z = 71$ , the Fermi level is the  $\alpha = 1/2$  routhian of  $i_{13/2}$  parentage in the frequency range  $250 \text{ keV} < \hbar\omega < 450 \text{ keV}$ . The lowest TSD band is observed in this frequency range and has  $(+, 1/2)$ . The lowest particle-hole (p-h) excitation of the same parity lifts the odd proton on to the other signature,  $\alpha = -1/2$ , of this  $i_{13/2}$  level, which lies at a relatively high energy ( $\sim 1 \text{ MeV}$  at  $\hbar\omega = 0.4 \text{ MeV}$ ). This brings the collective wobbling excitation, which has an excitation energy of about  $0.3 \text{ MeV}$ , well below the lowest p-h excitations. For  $Z = 69$ , however, the two signatures of the  $h_{11/2}$  state are quite close together (*cf.* Fig. 4). Therefore, the wobbling excitation lies above the p-h excitations, likely too high in excitation energy to be populated with observable strength in the  $(HI, xn)$  reaction employed in the present study. It is also worth mentioning that the relative energy of the collective wobbling mode and of the p-h excitations in  $^{163}\text{Lu}$  has been studied by means of the triaxial particle rotor model, where the p-h excitations have been called the “cranking mode” [12]. These are found to be located well above the one-phonon wobbling excitation. With the level order suggested in Fig. 6, one expects, for  $Z = 69$ , a band structure similar to the one seen in  $Z = 71$  at somewhat higher energy; it is obtained by lifting the last proton from the  $h_{11/2}$  into the  $i_{13/2}$  orbital. For  $Z = 73$ , several TSD bands of both parities with similar energy are expected.

The possibility to experimentally identify a wobbling band is restricted by the competition of this collective excitation with the p-h excitations. If the energy of the p-h excitations is high and the energy of the wobbling band is low, it may become the first excited band above the yrast line. Such a case appears to be realized in the Lu isotopes. The opposite occurs in  $^{163}\text{Tm}$ . The energy for the p-h excitations between the signature partners of the  $h_{11/2}$  orbital is much smaller than the wobbling energy. In the experiment, only the first

excited band, which corresponds to a p-h excitation, appears to have received sufficient intensity for observation. As seen in Fig. 6, the proton level density in the frequency range of 300-500 keV is larger for  $Z = 72$  and  $73$ . Moreover, we find that there is a gap at  $N = 94$  in the neutron diagrams, which prevents the neutron p-h excitations to compete with the wobbling mode in the Lu isotopes. Around  $N = 102-104$ , the density of neutron orbitals is high in the relevant frequency range. This means that, for these nuclides, many low-lying p-h excitations are possible, and it would be difficult to disentangle a collective wobbling structure from these many bands. Moreover, the wobbling mode is expected to be fractionated among the p-h excitations of the same parity. This would account for the presence of many strongly deformed bands in these nuclei [13, 14], none of which shows the characteristics of a wobbling mode. Based on this observation, Ref. [13] suggested that these nuclides might be less triaxial than the Lu isotopes. However, as discussed above, the apparent absence of a wobbling band does not necessarily imply a near-axial shape; indeed, that would be in contradiction with our calculations as well as with earlier ones [23].

In summary, two interacting strongly-deformed triaxial (TSD) bands have been observed in the  $Z=69$  nucleus  $^{163}\text{Tm}$ . This is the first observation of interacting TDS bands in an element other than Lu where wobbling bands have been identified. The observed TSD bands in  $^{163}\text{Tm}$  appear to correspond to particle-hole excitations, rather than to wobbling. Tilted Axis Cranking calculations reproduce all experimental observables for these bands reasonably well. The calculations also provide an explanation for the presence of wobbling bands in the Lu isotopes ( $Z = 71$ ) and their absence in the nearby Tm, Hf, and Ta isotopes ( $Z = 69, 72, 73$ ).

The authors express their gratitude to Drs. D. Ward, R.M. Clark, and P. Fallon for their invaluable assistance with the measurements with Gammasphere. This work has been supported in part by the U.S. National Science Foundation (Grants No. PHY04-57120 and INT-0111536), the Department of Science and Technology, Government of India (Grant No. DST-NSF/RPO-017/98), the U.S. Department of Energy, Office of Nuclear Physics, under contract No. W-31-109-ENG-38 and Grant DE-FG02-95ER40934 and the U.K. Science and Engineering Research Council.

---

[1] A. Bohr and B. Mottelson, *Nuclear Structure*, Vol. II (World Scientific, Singapore, 1998).

- [2] R. Bengtsson, H. Frisk, and F.R. May, Nucl. Phys. **A415** (1984) 189.
- [3] I. Hamamoto *et al.*, Phys. Lett. B **201** (1988) 415.
- [4] S. Frauendorf, Rev. Mod. Phys. **73** (2001) 463.
- [5] G.B. Hagemann and I. Hamamoto, Nucl. Phys. News **13** (2003) 20.
- [6] S.W. Ødegård *et al.*, Phys. Rev. Lett. **86** (2001) 5866.
- [7] D.R. Jensen *et al.*, Nucl. Phys. **A703** (1990) 3.
- [8] D.R. Jensen *et al.*, Phys. Rev. Lett. **89** (2003) 142503.
- [9] G. Schönwaßer *et al.*, Phys. Lett. B **552** (2003) 9.
- [10] H. Amro *et al.*, Phys. Lett. B **553** (2003) 197.
- [11] P. Bringel *et al.*, Eur. Phys. J A **24** (2005) 167.
- [12] D. R. Jenssen *et al.*, Eur. Phys. J A **19** (2004) 173.
- [13] D.J. Hartley *et al.*, Phys. Rev. C **72** (2005) 064325.
- [14] D.J. Hartley *et al.*, in *Nuclei at the Limits*, T.L. Khoo, D. Sewerennyak, and C. Lister, Editors (IOP Publishing, New York, 2005) pp 15.
- [15] I.-Y. Lee, Nucl. Phys. **A520** (1990) 641c.
- [16] N. S. Pattabiraman *et al.*, Nucl. Instr. Methods Phys. Res. **A526** (2004) 432; *ibid.* 439.
- [17] D. C. Radford, Nucl. Instr. and Methods Phys. Res. **A361** (1995) 297.
- [18] H.J. Jensen *et al.*, Z. Phys. A **340** (1991) 351.
- [19] X. Wang *et al.* (to be published).
- [20] T. Bengtsson and I. Ragnarsson, Nucl. Phys. **A436** (1985) 14.
- [21] S. Frauendorf, Nucl. Phys. **A677** (2000) 115.
- [22] A.V. Afanasjev, D.B. Fossan, G.J. Lane, and I. Ragnarsson, Phys. Rep. **322** (1999) 1.
- [23] R. Bengtsson and H. Ryde, Eur. Phys. J. A **22** (2004) 355.
- [24] W. Nazarewicz, M.A. Riley, and J.D. Garrett, Nucl. Phys. **A512** (1990) 61.
- [25] V.I. Dimitrov, F. Donau, and S. Frauendorf, Phys. Rev. C **62** (2000) 024315.